Original Article

Asian Pacific Journal of Tropical Biomedicine

journal homepage: www.apjtb.org

doi: 10.4103/2221-1691.328055

Impact Factor: 1.55

Crotalaria ferruginea extract attenuates lipopolysaccharide-induced acute lung injury in mice by inhibiting MAPK/NF-κB signaling pathways

Wei Pan[1,2#], Li-Ping Meng[3#], Jie Su[1], Zheng-Biao Yang[2], Wei-Feng Du[1], Zhi-Wei Xu[1], Yun-Xiang Chen[2], Sheng Zhang[2], Feng Xie[2], Cong Xu[2], Hong-Zhong Yang[2✉], Wei-Hong Ge[1#✉]

[1]*Department of Pharmacology, College of Pharmaceutical Sciences, Zhejiang Chinese Medical University, Hangzhou 310053, China*

[2]*State Key Laboratory of Safety Evaluation for New Drugs, Hangzhou Medical College, Hangzhou 310013, China*

[3]*Department of Surgical Nursing, The First Affiliated Hospital of Hainan Medical University, Haikou 570102, China*

ABSTRACT

Objective: To evaluate the anti-inflammatory activity of *Crotalaria ferruginea* extract (CFE) and its mechanism.

Methods: An intratracheal lipopolysaccharide (LPS) instillation-induced acute lung injury (ALI) model was used to study the anti-inflammatory activity of CFE *in vivo*. The LPS-induced shock model was used to analyze the effect of CFE on survival. LPS-stimulated RAW264.7 cell model was used to investigate the anti-inflammatory activity of CFE *in vitro* and the effects on mitogen-activated protein kinase (MAPK) or nuclear factor-κB (NF-κB) signaling pathways.

Results: CFE administration decreased the number of inflammatory cells, reduced the levels of tumor necrosis factor-α (TNF-α), monocyte chemotactic protein-1 (MCP-1), interleukin-6 (IL-6), and interferon-γ, and diminished protein content in the bronchoalveolar lavage fluid of mice. CFE also reduced lung wet-to-dry weight ratio, myeloperoxidase, and lung tissue pathological injury. CFE pre-administration improved the survival rate of mice challenged with a lethal dose of LPS. CFE reduced LPS-activated RAW264.7 cells to produce nitric oxide, TNF-α, MCP-1, and IL-6. Furthermore, CFE inhibited nuclear translocation and phosphorylation of NF-κB P65, extracellular signal-regulated kinase, c-Jun *N*-terminal kinases, and P38 MAPKs.

Conclusions: CFE exhibits potent anti-inflammatory activity in LPS-induced ALI mice, LPS-shock mice, and RAW264.7 cells, and its mechanism may be associated with the inhibition of NF-κB and MAPK signaling pathways. *Crotalaria ferruginea* may be a useful therapeutic drug for the treatment of ALI and other respiratory inflammations.

KEYWORDS: *Crotalaria ferruginea*; Acute lung injury; Cytokine; Lipopolysaccharide; Nuclear factor-κB; Mitogen-activated protein kinase

1. Introduction

Acute lung injury (ALI) is an acute and progressive pulmonary dysfunction caused by non-cardiogenic factors such as infection, trauma, shock, and inhalation of toxic agents[1]. Symptoms of ALI include pulmonary edema, hypoxemia, and dyspnea. However, even with prompt treatment, many ALI patients develop severe acute respiratory distress syndrome (ARDS) with a high mortality rate of 35%-50%[2,3]. Over-activated pulmonary inflammation that causes abnormal gas exchange function is the center of the pathology of ALI/ARDS[4–6]. Although considerable progress in understanding the pathogenesis and pathophysiology of ALI/ARDS has been made, the treatment remains limited.

The most important cause of ALI is bacterial sepsis, either as an independent factor or a combined factor. A high level of plasma lipopolysaccharide (LPS) was detected in sepsis patients[7].

✉To whom correspondence may be addressed. E-mail: geweihong12@163.com (Ge WH), yjl6875@163.com (Yang HZ)

#contributed equally to this manuscript.

How to cite this article: Pan W, Meng LP, Su J, Yang ZB, Du WF, Xu ZW, et al. *Crotalaria ferruginea* extract attenuates lipopolysaccharide-induced acute lung injury in mice by inhibiting MAPK/NF-κB signaling pathways. Asian Pac J Trop Biomed 2021; 11(11): 481-490.

Article history: Received 29 November 2020; Revision 4 January 2021; Accepted 27 August 2021; Available online 29 October 2021

Moreover, LPS, an important component of the cell walls of Gram-negative bacteria, stimulates inflammatory responses. ALI animal model induced by intratracheal LPS installation is widely applied, which well characterizes the pathological and inflammatory changes found in ALI patients[8]. Specifically, LPS activates macrophages and neutrophils to release inflammatory cytokines such as interleukin-6 (IL-6), tumor necrosis factor-α (TNF-α), monocyte chemotactic protein-1 (MCP-1), interferon-γ (IFN-γ), nitric oxide (NO), and myeloperoxidase (MPO) that are highly toxic to endothelial and epithelial cells. These mediators disrupt the alveolar-capillary membrane and cause lung edema and vascular leakage, dysfunction of gas exchange, and ultimately leading to lung failure[9].

Studies have demonstrated that LPS activates macrophages to release cytokines through nuclear factor-κB (NF-κB) and mitogen-activated protein kinase (MAPK) pathways. In particular, LPS binds to Toll-like receptors to activate MyD88 dependent pathways including MAPKs [extracellular signal-regulated kinase (ERK), c-Jun *N*-terminal kinases (JNK), and P38] and NF-κB[10]. It has been identified that NF-κB is activated by dissociating from inhibitor of kappa B (IκB) and then translocates from the cytoplasm to the nucleus[11]. Besides, NF-κB-DNA binding induces the expression of pro-inflammatory genes, such as IL-6, TNF-α, and nitric oxide synthase 2(NOS2)[12]. Meanwhile, MAPK signaling pathways are activated in LPS-induced ALI mice to stimulate cytokine production. Of note, the inhibition of NF-κB and MAPK signaling pathways may be a suitable strategy for the treatment of LPS-induced ALI[10].

Currently, herbal medicine has received great continuous research attention as an important source for drug discovery. *Crotalaria ferruginea* (*C. ferruginea*) Grah is a herb that is widely used in southwest China for the treatment of a variety of respiratory inflammatory disorders, for instance, cough, pneumonia, and asthma. It has been approved by Yunnan Province Food and Drug Administration as a medicine for respiratory infections and clearing heat and removing dampness[13]. This medical plant, whose main antibacterial constituents are flavonoids, exerts antibacterial activity against common pathogenic bacteria such as *Escherichia coli*, *Pseudomonas aeruginosa*, *Staphylococcus aureus*, and *Micrococcus luteus*[14,15]. Previous studies have isolated and characterized constituents of flavonoids from the herb, namely, genistein, kaempferol, quercetin, and stigmasterol, which possess inflammation-inhibitory activity[16–19]. *C. ferruginea* Grah has the potential to reduce the mouse pinna swelling induced by xylene as well as inhibit mice response to pain induced by the hot-plate or acetum stimulus[20]. However, there is no report about the activity of *C. ferruginea* Grah against respiratory inflammation. Therefore, we used the LPS-induced ALI mouse model and LPS-induced RAW264.7 cell model to systematically study the anti-inflammatory properties of *C. ferruginea* Grah in order to provide a valuable reference for this widely used resource.

2. Materials and methods

2.1. Reagents

LPS (*Escherichia coli* O55: B5) and 3-(4,5-dimethylthiazol-2-yl)-2,5-diphenyltetrazolium bromide (MTT) were purchased from Sigma-Aldrich (St. Louis, MO, USA). Dexamethasone sodium phosphate injection, cytometric bead array mouse inflammation cytokine kit, and MPO activity test kit were acquired from Baiyunshan Medicine Co, Ltd, China, BD Biosciences (New Jersey, USA), and Nanjing Jiancheng Bioengineering Institute (Nanjing, China), respectively. Additionally, p-P65, P65, p-P38, P38, p-ERK, ERK, p-JNK, and JNK antibodies were obtained from Cell Signaling Technology (Beverly, MA, USA). Finally, Griess reagent, BCA Protein Assay Kit, RIPA lysis buffer and protease and phosphatase inhibitor cocktail kits, α-tubulin, Lamin B3 antibodies as well as HRP-conjugated secondary antibody, DAPI, Triton X-100, and Alexa Fluor 488 IgG, nuclear and cytoplasmic protein extraction kit, were purchased from Beyotime Institute of Biotechnology (Jiangsu, China). All other chemicals used were of the analytical grade available.

2.2. Plant material

Raw plant materials were purchased from a traditional Chinese medicine market in Yunnan Province. The plant was identified as authentic by vice Prof. Wei-Feng Du, School of Pharmacy, Zhejiang University of Traditional Chinese Medicine (Hangzhou, China). A voucher specimen (AP201801) was deposited at the State Key Laboratory of Safety Evaluation for New Drugs, Hangzhou Medical College. The *C. ferruginea* Grah (500 g) was crushed and extracted using 70% ethanol (6 L×3 times) at room temperature for 24 h each time, followed by filtration and concentration in vacuo, eventually yielding a brownish extract with a mass-weight of 75.2 g. The standard substance of genistein was obtained from Chengdu Must Biotechnology Co, Ltd, China.

2.3. HPLC analysis of genistein in C. ferruginea extract (CFE)

Using an HPLC system (Agilent Technologies, USA) equipped with a Synersi C 18 column (250 mm×4.6 mm, 5 μm, Phenomenex), we determined genistein in the CFE according to a previously described method with minor modifications[15]. The mobile phase used was composed of acetonitrile (A) and 1% acetic acid (B). The gradient program was set as follows: 63% B (0-4.5 min), 63%-52% B (4.5-13 min), 52%-37% B (13-13.10 min), 37% B (13.10-20 min). The column temperature was maintained at 30℃, while the mobile phase flow rate was 1 mL/min. The measured absorbance wavelength was 260 nm, whereas the injection volume was 20 μL.

2.4. Evaluation of anti-inflammatory property in mice

2.4.1. Animals

Specific-pathogen-free female ICR mice (18-22 g, 6-8 weeks) were obtained from Shanghai Slack Laboratory Animal Co. Ltd. The mice were maintained in a barrier system with laboratory temperature maintained at 20-25℃, 50%-70% relative humidity, and under a 12 h:12 h light: dark cycle. They were housed in micro isolator cages and were provided food and water *ad libitum*.

2.4.2. Animal experiment design

Overall, 60 female mice were randomly divided into 6 groups, namely: control, LPS, CFE (0.25, 0.5, and 1 g/kg) + LPS, and dexamethasone (0.5 mg/kg, positive control) + LPS groups with 10 mice in each group. The mostly used dose of *C. ferruginea* on an adult (60 kg) was 20 g once. According the conversion relationship between human and mice, the corresponding equivalent dose for mice was calculated to be 3.6 g/kg body weight, equal to the CFE extract dose was 0.5 g /kg. This dose was set as middle dose in mice and the high dose and low dose were set as 1.0 g/kg and 0.25 g/kg, respectively. On days 1-7, experimental mice in the control group received oral administration of saline, while the CFE + LPS group received the designated dose of CFE. On day 7, dexamethasone + LPS group mice were given a single dose of 0.5 mg/kg dexamethasone intraperitoneally. All mice were anesthetized by intraperitoneal administration with 0.5% pentobarbital (30 mg/kg) and intratracheally administrated with 20 μg LPS in 50 μL saline except the control group, which was given the same volume of saline[21]. On day 8, mice were sacrificed and the right lung was ligated and removed. The right upper lung was used to obtain the lung wet-to-dry weight ratio (W/D ratio), while the right middle lung was homogenized to detect MPO activity.

2.4.3. Differential cell counts and analysis of cytokine, protein levels in bronchoalveolar lavage fluid (BALF)

The mouse tracheae were surgically isolated and intubated with a 24-gauge cannula. BALF was collected by cannulating the trachea and infusing the left lung of mice thrice with 0.5 mL ice-cold saline *via* intratracheal cannulation. Then, the BALF samples were centrifuged at 2000 rpm for 5 min at 4℃. Upon resuspending cells in saline, the total cells were counted using a hemacytometer, while the differential leukocyte count was performed using Wright–Giemsa staining. BALF supernatant was stored at –80℃ until the cytokine levels were detected with a mouse inflammation kit (BD™ Cytometric Array, USA) using the flow cytometer (BD FACS Calibur™, USA). Lastly, we measured protein contents in BALF using the bicinchoninic acid (BCA) method with a microplate reader (Biotek synergy, USA).

2.4.4. Lung W/D ratio and MPO activity

To assess the lung edema degree, we excised and weighted the lower lobe of the right lung. Then, the lungs were dried in an oven at 80℃ for 48 h to obtain lung dry weight. The lung W/D ratio was calculated to indicate lung edema. The level of lung MPO activity was determined using a colorimetric assay kit with a microplate reader (Biotek Synergy) as per the manufacturer's instructions.

2.4.5. Histopathologic evaluation of the lung tissue

The lower right lung was fixed with 10% buffered formalin for 48 h at room temperature and embedded in paraffin. Then, tissue sections were cut at 4 μm thickness, stained with hematoxylin and eosin, and scored for lung injury by two independent experienced pathologists based on the criteria described elsewhere[10]: 0 = minimal (<1%); 1 = slight (1%-25%); 2 = moderate (26%-50%); 3 = moderate/severe (51%-75%); and 4 = severe/high (76%-100%).

2.5. Endotoxin shock survival test

For endotoxin shock research, a total of 30 female ICR mice were divided into three groups (n=10 per group). These included (A) LPS group, (B) LPS + CFE 0.25 g/kg, and (C) LPS + CFE 1 g/kg. The mice of A, B, and C groups received saline and CFE 0.25 or 1 g/kg for 7 d. On day 7, 1 h after the last administration, the ICR mice were intraperitoneally injected with 50 mg/kg LPS (0.2 mL/10 g body weight, dissolved in saline). The survival of mice was monitored for 5 d[22].

2.6. Cell viability

MTT cell viability assay was used to evaluate the cytotoxicity of CFE. The RAW264.7 cells (Gefan Biotechnology Co. Ltd, China) were seeded in 96 well plates at a density of 5×10^5 cells/mL for 24 h and treated with CFE at different concentrations of 25-400 μg/mL for 24 h, the supernatant was discarded, followed by the addition of 0.5 mg/mL MTT. After 4 h, 100 μL DMSO was added to dissolve formazan crystals. Finally, the optical density value was quantified using a microplate reader (Biotek synergy, USA) at 570 nm.

2.7. Measurement of NO, cytokine production in RAW264.7 supernatant

The amount of NO release was quantified in the form of nitrite production. RAW264.7 cells were seeded in 96 well plates at a concentration of 5×10^4 cells/well, pretreated with different concentrations of CFE (50, 100, 200 μg/mL) for 2 h, followed by LPS (1 μg/mL) administration for 18 h. Briefly, the culture media were collected, mixed with an equal volume of Griess reagent, and incubated at room temperature for 10 min. $NaNO_2$ was used to generate a standard curve, and nitrite production was ascertained by measuring the absorbance at 540 nm. The cytokines in the supernatant of RAW264.7 cells were analyzed with a mouse

inflammation kit using a flow cytometer. Three independent experiments were performed (n=6).

2.8. Immunofluorescence

For this technique, RAW264.7 cells were seeded in 6 well plates at a density of 5×10^4 cells/well and left overnight. Cells were pretreated with CFE (200 μg/mL) for 24 h and then stimulated with LPS (1 μg/mL) for 15 min. The cells were washed twice with cold PBS, fixed with 4% formaldehyde for 15 min, and then permeabilized in 0.5% Triton X-100 for 15 min. Upon blocking with goat serum for 30 min at room temperature, the cells were incubated with primary anti-P65 antibody overnight at 4 ℃ and then stained with secondary antibody (Alexa Fluor 488 IgG) for 1 h. The nuclei were labeled with DAPI for 15 min in the dark. Lastly, the cells were observed under a fluorescence microscope (Leica DM4000B, Wetzlar, Germany) at an excitation wavelength of 364 nm for DAPI and 495 nm for Alexa Fluor 488[22].

2.9. Western blot analysis

RAW264.7 cells were seeded in 6 well plates (1×10^6 cells/well), pretreated with different concentrations of CFE (50, 100, 200 μg/mL) for 24 h, followed by LPS (1 μg/mL) administration for 30 min. Cells in 6 well plates were washed with cold PBS three times, the cells were lysed with RIPA buffer and a protease and phosphatase inhibitor cocktail (Beyotime shanghai China), and then centrifuged at 12 000 rpm for 15 min at 4 ℃. Protein concentrations were determined by the BCA assay. The same mass of total protein was loaded per well on 12% SDS-polyacrylamide gels with α-tubulin, GAPDH, or Lamin B3 as internal loading control. After gel transfer, PVDF membranes were blocked with 5% free-fat milk for 1 h at room temperature and incubated overnight at 4 ℃ with primary antibodies to p-P65, P65, p-P38, P38, p-ERK, ERK, p-JNK, JNK (1:1 000), then the membranes were incubated with secondary antibodies (1:2 000) for 1 h. The protein bands were detected with an enhanced chemiluminescence method, and the fluorescence intensity was calculated using ImageJ software (National Institutes of Health, USA).

2.10. Statistical analysis

Statistical analysis was performed by GraphPad Prism 5 (GraphPad Software, Inc.). Data were expressed as mean ± standard deviation (mean ± SD). Differences between groups were analyzed by one-way analysis of variance (ANOVA) to work out the F value first. When F-value was significant, *post hoc* analysis (Tukey's test) was performed. A P-value < 0.05 was considered statistically significant.

2.11. Ethical statement

Study protocol was conducted in accordance with the Animal Care and Use Committee of Hangzhou Medical College guidelines, approved by the Ethics Committee of State Key Laboratory of Safety Evaluation for New Drugs on December 6, 2019 (No. KY-2019-10).

3. Results

3.1. HPLC analysis of genistein in CFE

HPLC analysis of chemical compounds in ethanol extract of *C. ferruginea* showed the presence of flavonoid monomers. Notably, the retention time was 16.20 min (Figure 1), the content of genistein was 0.68 mg/g in CFE.

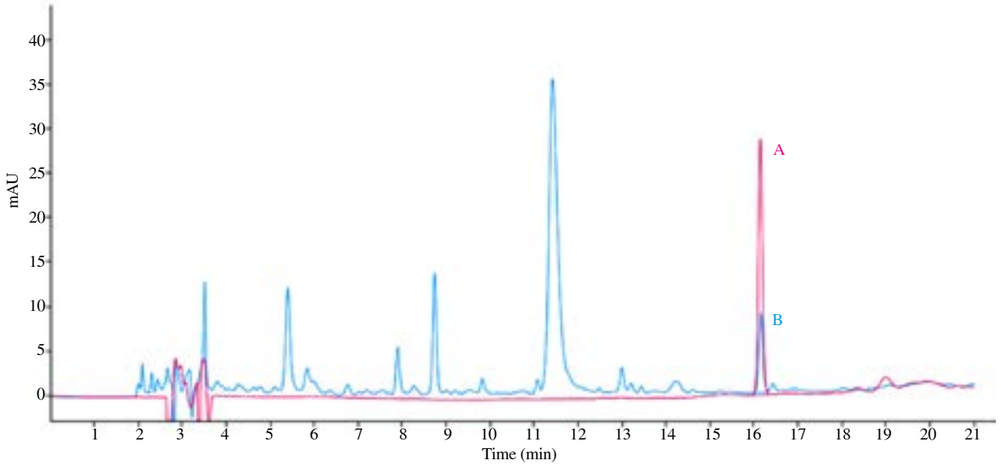

Figure 1. The HPLC chromatogram detected at 260 nm from (A) standard substance of genistein and (B) *Crotalaria ferruginea* extract (CFE).

3.2. Effect of CFE on inflammatory cell infiltration in LPS-induced ALI mice

To identify CFE anti-inflammatory activity, cell count and classification in BALF were analyzed. We noted that the total number of BALF cells in model group mice increased after the LPS challenge compared to the control group, indicating significant recruitment of leukocytes into the alveolar space. In addition, CFE or dexamethasone decreased total leukocyte cell number, neutrophil, and macrophage number in BALF (P<0.05, Figures 2A-C). MPO is a marker of neutrophil activation and degree of inflammation. Notably, the activity of MPO was greater in LPS-treated mice than in the control group mice. On the other hand, MPO activity was reduced in dexamethasone as well as in the middle and high-dose CFE groups (P<0.01, Figure 2D).

3.3. Effects of CFE on inflammatory mediator levels in BALF from LPS-induced mice

The inflammatory mediators, namely IL-6, MCP-1, TNF-α, and IFN-γ in BALF of model group mice increased after the LPS challenge compared to the control group. Our findings revealed that CFE (0.25, 0.5, 1 g/kg) or dexamethasone inhibited the IL-6, MCP-1, TNF-α, and IFN-γ in BALF release induced by LPS intratracheal instillation (P<0.05, Figure 3).

3.4. Effects of CFE on lung W/D ratio and protein concentration in BALF

Here, the lung W/D ratio and protein concentration in BALF were examined to assess the LPS induced changes in alveolar-capillary membrane permeability. Pulmonary edema in LPS-induced ALI

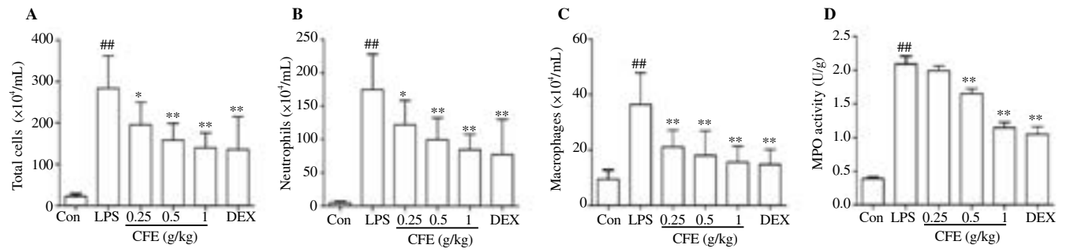

Figure 2. Effect of CFE on inflammatory cell infiltration in lipopolysaccharide (LPS)-induced acute lung injury (ALI) mice. (A-C) The number of total cells, neutrophils, and macrophages in the bronchoalveolar lavage fluid (BALF). (D) Myeloperoxidase (MPO) activity of lung tissue. $^{*}P$<0.05 and $^{**}P$<0.01 *vs.* the LPS group, $^{\#\#}P$<0.01 *vs.* the control group. n=10 in each group. Con: control group; DEX: Dexamethasone.

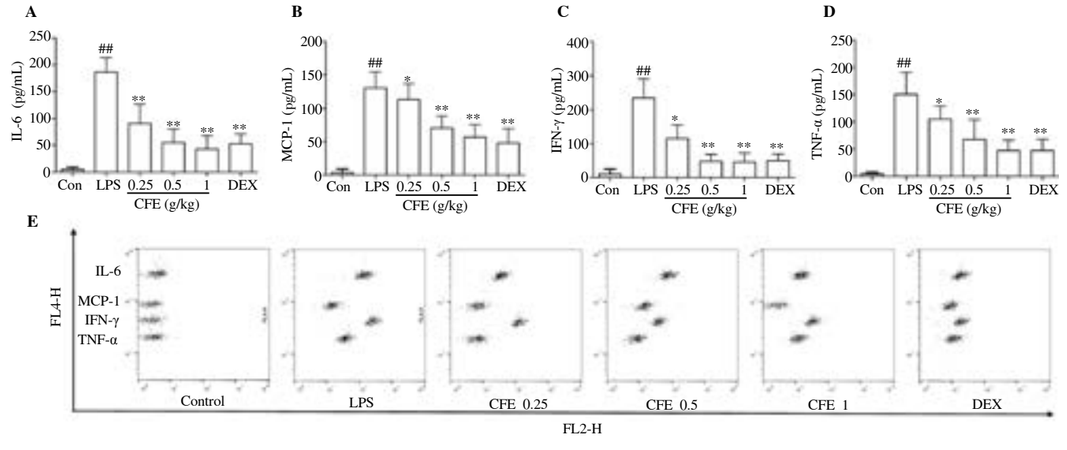

Figure 3. Inhibitory effect of CFE on LPS-stimulated production of pro-inflammatory cytokines. (A-D) Levels of interleukin-6 (IL-6), monocyte chemotactic protein-1 (MCP-1), interferon-γ (IFN-γ), and tumor necrosis factor-α (TNF-α) in BALF, respectively. (E) Representative flow cytometry plots showing BALF cytokine levels. $^{*}P$<0.05 and $^{**}P$<0.01 *vs.* the LPS group, $^{\#\#}P$<0.01 *vs.* the control group. n=10 in each group.

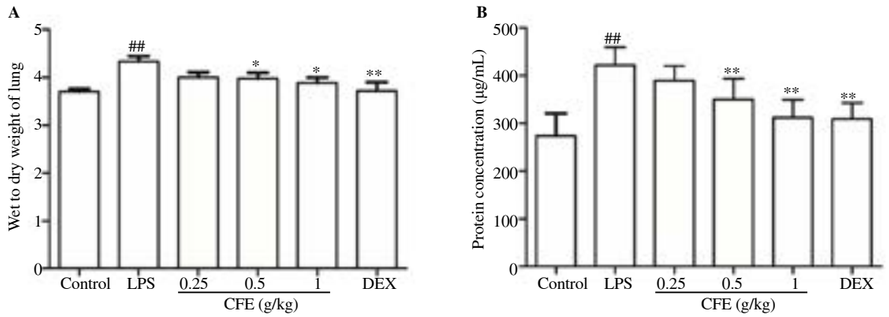

Figure 4. Effect of CFE on the ratio of lung wet to dry weight and protein level in BALF. (A) Measurement of pulmonary edema as the ratio of lung wet to dry weight. (B) The protein concentration in BALF. $^{*}P<0.05$ and $^{**}P<0.01$ *vs.* the LPS-treated group, $^{\#\#}P<0.01$ *vs.* the control group. $n=10$ in each group.

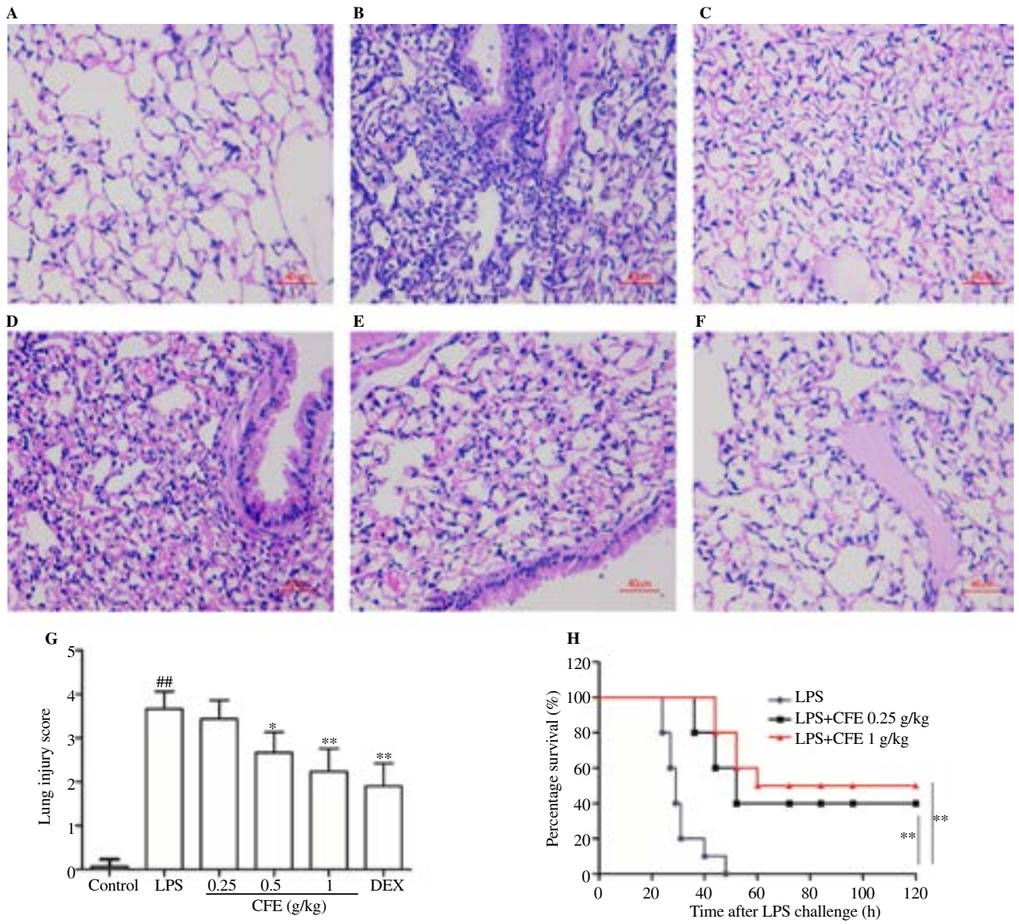

Figure 5. Effect of CFE on pathological changes in LPS-induced ALI mice. (A-F) The figure shows a representative view from each group (scale bar: 40 μm). (A) Control group; (B), LPS group; (C), LPS + dexamethasone 0.5 mg/kg; (D), LPS + CFE 0.25 g/kg, (E), LPS + CFE 0.5 g/kg; and (F), LPS + CFE 1 g/kg. (G) Quantitative histological assessment using lung injury score. $n=10$ in each group. (H) The survival curves are drawn using the Kaplan-Meier method and compared with the log-rank statistic ($P<0.01$). $^{*}P<0.05$ and $^{**}P<0.01$ *vs.* the LPS-treated group, $^{\#\#}P<0.01$ *vs.* the control group. $n=10$ in each group.

mice was measured as W/D ratio. The results showed that the lung W/D ratio increased in the LPS-induced model mice, while CFE (0.5, 1 g/kg) or dexamethasone pre-treatment decreased the W/D ratio significantly ($P<0.05$, Figure 4A). BALF protein content, which reflects pulmonary vasculature permeability, was elevated after LPS stimulation. Furthermore, mice that were given CFE (0.5, 1 g/kg) or dexamethasone exhibited lower BALF protein levels than the LPS group, meaning that the alveolar-capillary membrane integrity was protected ($P<0.01$, Figure 4B).

3.5. Effects of CFE on lung histopathological changes in LPS-induced ALI mice

Lung histopathology results of mice in the control group showed alveolar structural integrity and clear alveolar cavity without inflammatory cell infiltration. Neutrophils and macrophages infiltration, alveolar wall thickening, and alveolar hemorrhage in the lung of LPS-treated mice appeared to a larger extent than in the control group (Figures 5A-F). Notably, CFE (0.5, 1 g/kg) treatment improved the above pathological changes in a dose-dependent manner, leading to reduced lung injury scores ($P<0.05$, Figure 5G). Positive drug dexamethasone can partly alleviate pathological damage. The Kaplan–Meier survival curve of endotoxemic mice in all three groups (LPS group, LPS + CFE 0.25 g/kg, LPS + CFE 1 g/kg) was drawn. Finally, CFE (0.25, 1 g/kg) treatment profoundly prolonged the survival compared to the animals pretreated with saline, and the highest dose possessed greater protective capacity ($P<0.01$, Figure 5H).

3.6. Effects of CFE on the LPS-induced IL-6, MCP-1, TNF-α, and NO in RAW264.7 cells

CFE at 400 μg/mL maximum concentration for 24 h exhibited no toxicity on RAW264.7 cells according to the MTT test (Figure 6A). Therefore, the concentrations of CFE at 50, 100, and 200 μg/mL were selected for the following experiments to avoid the cytotoxic effect on the RAW264.7 cells. The concentrations of inflammatory mediators were low or undetectable in the control group. The levels of NO, IL-6, MCP-1, and TNF-α in cell culture supernatants increased significantly after LPS stimulation, while the pre-treatment of CFE suppressed these inflammatory cytokines release in a concentration-dependent manner ($P<0.01$). Collectively, these findings demonstrate that CFE had an anti-inflammatory effect against LPS-induced stress in RAW264.7 macrophages (Figures 6B-F).

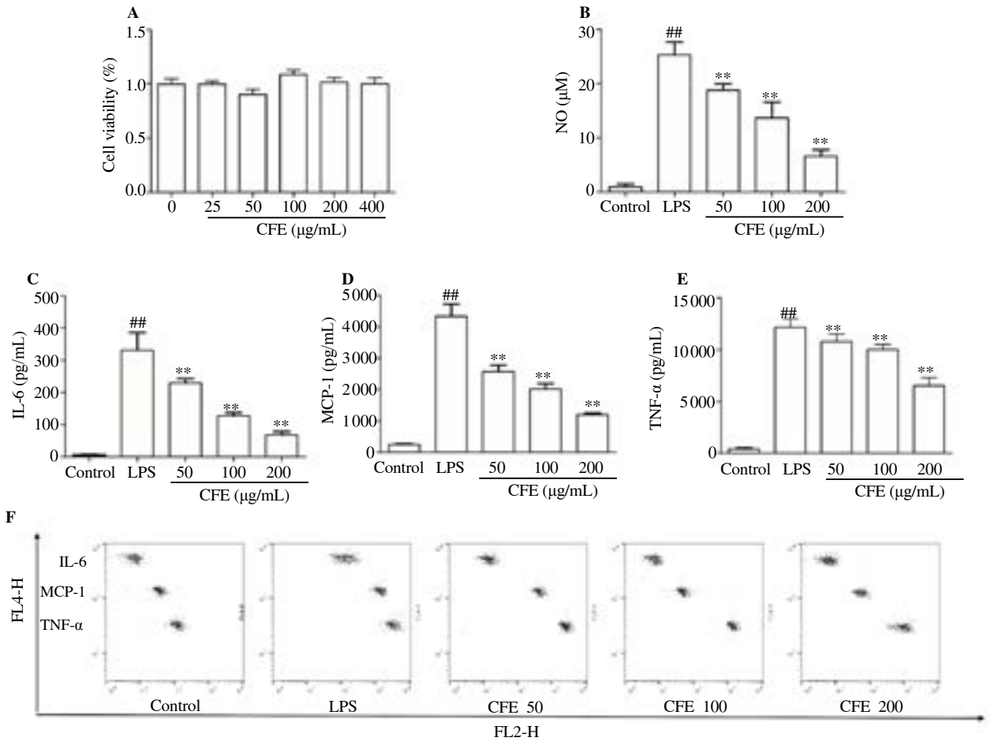

Figure 6. Effect of CFE on cytokine production in LPS-induced RAW264.7 cells. (A) Cell viabilities were evaluated using MTT assay. (B-E) NO, IL-6, MCP-1, and TNF-α in the supernatant of RAW264.7 cells. (F) Representative flow cytometry plots showing cytokine levels of cell culture supernatants. $^{**}P<0.01$ *vs.* the LPS-treated group, $^{\#\#}P<0.01$ *vs.* the control group. $n=10$ in each group.

3.7. Effects of CFE on the activities of NF-κB and MAPK signaling in RAW264.7 cells

To explore the inhibitory effects of CFE on the nuclear translocation of NF-κB, the immunofluorescence analysis was performed. After RAW264.7 cells were stimulated by LPS, the fluorescence intensity of P65 NF-κB in the nucleus was increased, implying the translocation of P65 from the cytoplasm to the nucleus. Remarkably, the CFE treatment (200 μg/mL) reduced the fluorescence intensity of P65 NF-κB in the nucleus (Figure 7A). In order to further confirm the effect of CFE on LPS-induced nuclear translocation of NF-κB in RAW264.7 macrophages, the nuclear and cytoplasmic proteins of RAW264.7 cells were extracted, the level of NF-κB P65 in nucleus and cytoplasm was detected by Western blotting. The level of P65 in the nucleus increased significantly and P65 level in the cytoplasm decreased significantly 30 min after LPS stimulation, indicating that P65 transferred from the cytoplasm into the nucleus. After RAW264.7 macrophages were treated with varying concentrations of CFE (50, 100, 200 μg/mL), the decrease of P65 level in the nucleus and the increase of P65 level in the cytoplasm indicated that

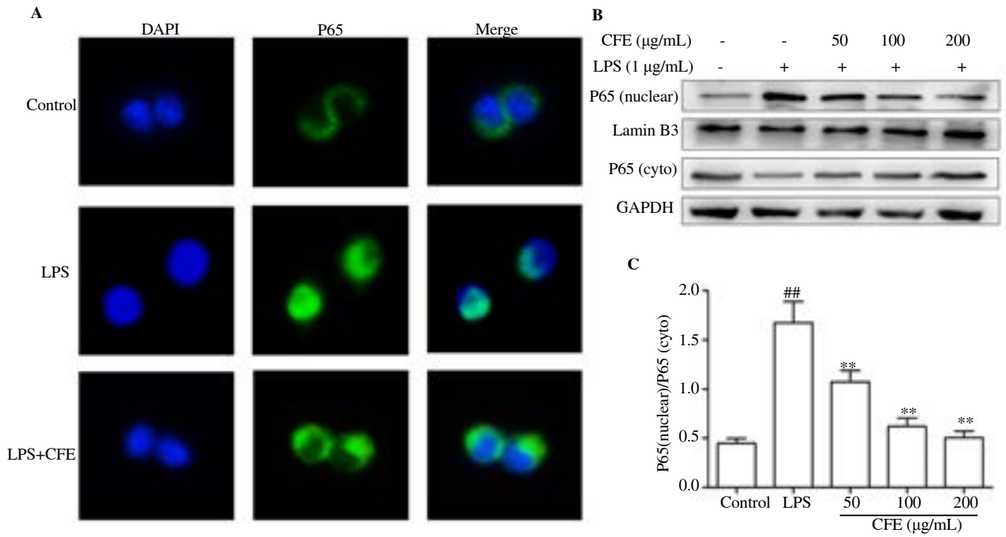

Figure 7. Effect of CFE on the LPS-induced nuclear factor-κB (NF-κB) P65 nuclear translocation. (A) RAW264.7 macrophages were pre-treated with CFE (200 μg/mL) for 24 h, and NF-κB P65 nuclear translocation was analyzed by immunofluorescence microscopy. Immunoreactivity of NF-κB P65 is shown in green, while the nuclei are stained with DAPI in blue. (B) Nuclear and cytoplasmic P65 levels were examined by Western blotting assays. (C) Ratios of nuclear P65/cytoplasm (cyto) P65 were quantified by densitometry using ImageJ software. Data from three independent experiments are shown. $^{\#\#}P<0.01$ *vs.* the control group. $^{**}P<0.01$ *vs.* the LPS-treated group.

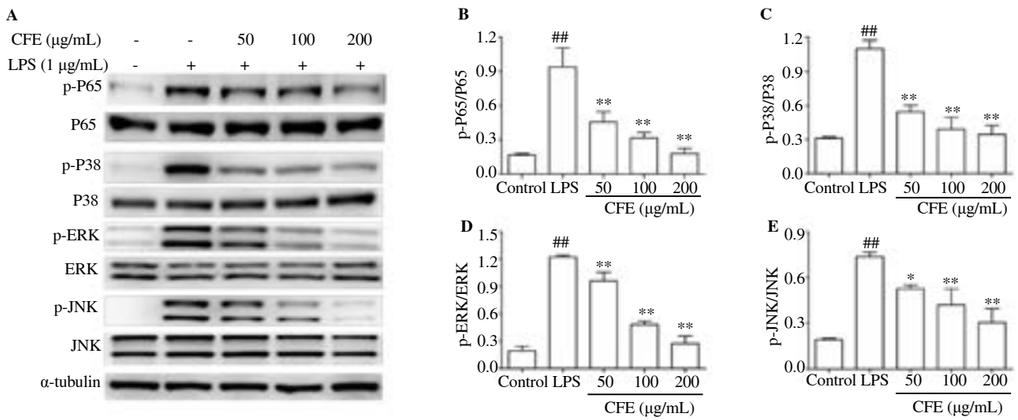

Figure 8. Effects of CFE on the LPS-induced phosphorylation of NF-κB P65 and mitogen-activated protein kinases (MAPKs) in RAW264.7 macrophages. (A) Total and phosphorylated P65, P38, extracellular signal-regulated kinase (ERK), and c-Jun *N*-terminal kinases (JNK), were measured by Western blotting assays. (B-E) Ratios of p-P65/P65, p-P38/P38, p-ERK/ERK, and p-JNK/JNK were quantified by densitometry using ImageJ software. Data from three independent experiments are presented. $^{\#\#}P<0.01$ *vs.* the control group. $^{*}P<0.05$, $^{**}P<0.01$ *vs.* the LPS-treated group.

the transfer of NF-κB P65 from the cytoplasm to the nucleus was inhibited (Figures 7B-C).

To probe the involved mechanism by which CFE decreases the production of inflammatory cytokines, the phosphorylation of NF-κB and MAPK pathway molecules was measured using Western blot analysis (Figure 8A). The results revealed that phosphorylation of p-P65, as a marker of NF-κB activation, was inhibited markedly, indicating that CFE can reduce inflammation by inactivating the NF-κB signaling pathway ($P<0.01$, Figure 8B). As denoted in Figures 8C-E, the phosphorylation of P38, ERK, and JNK was suppressed by CFE in a concentration-dependent pattern ($P<0.05$).

4. Discussion

In this study, we explored the effects of CFE on ALI model mice induced by intratracheal LPS instillation. We also evaluated the anti-inflammatory effects of CFE while dexamethasone was used as a positive control. The findings uncovered that the administration of CFE significantly improved the number of inflammatory cells infiltration, alveolar hemorrhage, protein leakage in BALF, the degree of pulmonary edema, and MPO levels in the lung injury mice. Additionally, CFE treatment protected LPS-induced pulmonary tissue injury in mice, as well as reduced mortality in mice treated with endotoxin (LPS) which highlighted its beneficial effect in the inflammation-associated disorders. Recent reports have enumerated that CFE significantly reduced xylene-induced ear swelling and acetic acid-induced writhing response in mice, indicating that CFE possessed anti-inflammatory and anti-nociceptive activity[20].

Cytokines including TNF-α, IL-6, MCP-1, and IFN-γ are important in the development of lung inflammation in LPS-induced injury[5]. When LPS-induced ALI occurs, macrophages are activated to secrete cytokines. Herein, we noted that the levels of TNF-α, MCP-1, IL-6, and IFN-γ increased in BALF from mice after intra-tracheal LPS installation to induce ALI, which is consistent with the previous reports[23]. Elsewhere, TNF-α stimulates vascular endothelial cells to express vascular cell adhesion molecule-1 to induce neutrophil recruitment and tight adhesion[24], whereas MCP-1 recruits neutrophils to penetrate the endothelial barrier to migrate and reside in the pulmonary interstitium and alveoli[25]. As a result, activated neutrophils release MPO during the degranulation process, eventually causing lung tissue damage[26]. IL-6 is capable of inhibiting the apoptosis of neutrophils as well as promoting the activation of neutrophils and macrophages, thus plays a key role in modulating acute and chronic inflammation[27]. Moreover, IFN-γ induces nitric oxide synthase 2 and secretes pro-inflammatory cytokines, hence enhancing the macrophage NO release and inflammatory response. In this work, our results outlined that CFE can reduce TNF-α, IL-6, IFN-γ, and MCP-1 levels in the BALF of LPS-induced mice. Furthermore, CFE inhibited the production of pro-inflammatory cytokines, namely, TNF-α, IL-6, and MCP-1 in LPS-stimulated RAW264.7 cells. This accords with the findings of the animal test. Therefore, we suggest that the protective effect of CFE on the ALI induced by LPS in mice may be ascribed to the inhibition of macrophage inflammatory response.

According to the literature on the development of ALI, the NF-κB and MAPK signaling pathways play a significant role in regulating the inflammation reaction process[28]. However, excessive activation of these signaling pathways may induce an inflammation response. In particular, NF-κB is a nuclear transcription factor that regulates immune-inflammatory response, which is usually inactive, existing in the cytoplasm of resting cells, and binding to the IκB. After stimulation by LPS, IκB-α is phosphorylated, releasing NF-κB P65. Activated NF-κB translocates to the nucleus, transcripts a variety of inflammatory cytokine genes such as TNF-α, MCP-1, and IL-6, which induce inflammation and then promote the development of ALI. In this study, after LPS stimulation in RAW264.7 cells, the NF-κB nuclear translocation and phosphorylation levels increased, which concurs with the literature. In addition, CFE treatment significantly reduced the phosphorylation levels of NF-κB in a concentration-dependent manner, signifying that CFE can inhibit the NF-κB pathway. Elsewhere, studies have elucidated that MAPK signaling pathway plays an imperative role in the pro-inflammatory reaction[29]. The activation of the MAPK pathway increases the release of pro-inflammatory cytokines. This pathway comprises extracellular regulated kinases (ERK1/2), P38 MAPKs, and JNK. Consistent with previous findings, we observed that the phosphorylation of JNK, ERK1/2, and P38 MAPK was significantly elevated after LPS stimulation. Finally, CFE treatment decreased p-JNK, p-ERK1/2, and p-P38 MAPK levels, therefore indicating that CFE can inhibit the MAPK pathway. In the previous research on the mechanism of protective effect of th drug against LPS-induced acute lung injury, the MAPK/NF-κB inhibition is consistent with our results. The upstream signaling transducer of MAPK/NF-κB like TLR4, MyD88, TRAF6, and negative regulator like A20, DUSP1 were investigated[30,31], which deserves our subsequent exploration on *C. ferruginea*.

In conclusion, this work demonstrates that CFE exhibited strong anti-inflammatory activity in LPS-induced mice. The involved anti-inflammatory mechanism may be associated with the inhibition of the NF-κB and MAPK signaling pathways.

Conflict of interest statement

The authors declare no conflict of interest.

Funding

This work was supported by the Natural Science Foundation of Zhejiang province (Grant LQ19H280009); Special Projects of Zhejiang Academy of Medical Sciences (Grant CA1918D-04, CA1903Q-04); Medical Health Science and Technology Project of Zhejiang Provincial Health Commission (Grant 2020384536).

Authors' contributions

WP and LPM contributed to data analysis and the final version of the manuscript. ZBY and WFD prepared and analyzed the ethanol

extract of *Crotalaria ferruginea*. JS, YXC, and ZWX performed all animal experiments. SZ, CX, and FX performed all cell experiments. WHG and HZY designed the study, and supervised all the experiments.

References

[1] Matthay M, Zemans R, Zimmerman G, Arabi Y, Beitler J, Mercat A, et al. Acute respiratory distress syndrome. *Nat Rev Dis Primers* 2019; **5**(18): 1-22.

[2] Fan E, Brodie D, Slutsky A. Acute respiratory distress syndrome: Advances in diagnosis and treatment. *JAMA* 2018; **319**(7): 698-710.

[3] Standiford TJ, Ward PA. Therapeutic targeting of acute lung injury and acute respiratory distress syndrome. *Transl Res* 2016; **167**(1): 183-191.

[4] Chen X, Tang J, Shuai W, Meng J, Feng J, Han Z. Macrophage polarization and its role in the pathogenesis of acute lung injury/acute respiratory distress syndrome. *Inflamm Res* 2020: **69**(9): 883-895.

[5] Bhatia M, Moochhala S. Role of inflammatory mediators in the pathophysiology of acute respiratory distress syndrome. *J Pathol* 2004; **202**(2): 145-156.

[6] Wong JJM, Leong JY, Lee JH, Albani S, Yeo JG. Insights into the immuno-pathogenesis of acute respiratory distress syndrome. *Ann Transl Med* 2019; **7**(19): 504.

[7] Opal SM, Scannon PJ, Jean-Louis V, Mark W, Carroll SF, Palardy JE, et al. Relationship between plasma levels of lipopolysaccharide (LPS) and LPS-binding protein in patients with severe sepsis and septic shock. *J Infect Dis* 1999; **180**(11): 1584-1589.

[8] Chen H, Bai C, Wang X. The value of the lipopolysaccharide-induced acute lung injury model in respiratory medicine. *Expert Rev Respir Med* 2010; **4**: 773-783.

[9] Nova Z, Skovierova H, Calkovska A. Alveolar-capillary membrane-related pulmonary cells as a target in endotoxin-induced acute lung injury. *Int J Mol Sci* 2019; **20**(4): 831-850.

[10]Wu KC, Huang SS, Kuo YH, Ho YL, Yang CS, Chang YS, et al. Ugonin M, a *Helminthostachys zeylanica* constituent. prevents LPS-induced acute lung injury through TLR4-mediated MAPK and NF-kappaB signaling pathways. *Molecules* 2017; **22**(4): 573-587.

[11]Sasaki CY, Barberi TJ, Ghosh P, Longo DL. Phosphorylation of RelA/p65 on serine 536 defines an IκB -independent NF-κB pathway. *J Biol Chem* 2005; **280**(41): 34538-34547.

[12]Tak PP, Firestein GS. NF-kappaB: A key role in inflammatory diseases. *J Clin Invest* 2001; **107**(1): 7-11.

[13]FDA Yunnan Province. *Standard of traditional Chinese medicine in Yunnan Province.* Kunming Yunan: Yunnan Science and Technology Press; 2007, p. 73-74.

[14]Wu ZJ, Zhou Y, Lu GF, Wang H, and Wang HJ. Antibacterial activity of flavonoid extracts from *Crotalaria ferruginea* Grah. *Guizhou Agric Sci* 2009; **37**(5): 83-84.

[15]Tang Q, Yang X, Liu Y, Wang B, Zhang X. Determination and content changes of total flavonoids and three flavonoid aglycones in *Crotalaria ferruginea* Grah. *Chem Ind Forest Prod* 2010; **30**(30): 93-98.

[16]Chen X, Yang X, Liu T, Guan M, Feng X, Dong W, et al. Kaempferol regulates MAPKs and NF-κB signaling pathways to attenuate LPS-induced acute lung injury in mice. *Int Immunopharmacol* 2012; **14**(2): 209-216.

[17]Antwi AO, Obiri DD, Osafo N. Stigmasterol modulates allergic airway inflammation in guinea pig model of ovalbumin-induced asthma. *Mediators Inflamm* 2017; **2017**: 2953930.

[18]Hooshmand S, Soung do Y, Lucas EA, Madihally SV, Levenson CW, Arjmandi BH. Genistein reduces the production of proinflammatory molecules in human chondrocytes. *J Nutr Biochem* 2007; **18**(9): 609-614.

[19]Wang XF, Song SD, Li YJ, Hu ZQ, Zhang ZW, Yan CG, et al. Protective effect of quercetin in LPS-induced murine acute lung injury mediated by cAMP-Epac pathway. *Inflammation* 2018; **41**(3): 1093-1103.

[20]Xia YB, Li LZ, Ma L, Yang XS, Hao XJ. Confirming the effective fraction of *Crotalaria ferruginea* on anti- inflammatory and analgesia with methods establishing for quality control. *J Chin Pharm Sci* 2010; **30**(9): 1599-1603.

[21]Wei J, Chen G, Shi X, Zhou H, Liu M, Chen Y, et al. Nrf2 activation protects against intratracheal LPS induced mouse/murine acute respiratory distress syndrome by regulating macrophage polarization. *Biochem Biophys Res Commun* 2018; **500**(3): 790-796.

[22]Yu WW, Lu Z, Zhang H, Kang YH, Mao Y, Wang HH, et al. Anti-inflammatory and protective properties of daphnetin in endotoxin-induced lung injury. *J Agric Food Chem* 2014; **62**(51): 12315-12325.

[23]Li LL, Zhang S, Xin YF, Sun JY, Xie F, Yang L, et al. Confirming the effective fraction of *Crotalaria ferruginea* on anti-inflammatory and analgesia with methods establishing for quality control. *J Chinese Pharm Sci* 2010; **30**(9): 1599-1603.

[24]Iademarco MF, Barks JL, Dean DC. Regulation of vascular cell adhesion molecule-1 expression by IL-4 and TNF-alpha in cultured endothelial cells. *J Clin Invest* 1995; **95**(1): 264-271.

[25]Bianconi V, Sahebkar A, Atkin SL, Pirro M. The regulation and importance of monocyte chemoattractant protein-1. *Curr Opin Hematol* 2018; **25**(1): 44-51.

[26]Colgan SP. Neutrophils and inflammatory resolution in the mucosa. *Semin Immunol* 2015; **27**(3): 177-183.

[27]Choy E, Rose-John S. Interleukin-6 as a multifunctional regulator: Inflammation, immune response, and fibrosis. *J Scleroderma Relat Disord* 2017; **2**(2 Suppl): S1-S5.

[28]Liu S, Feng G, Wang GL, Liu GJ. p38MAPK inhibition attenuates LPS-induced acute lung injury involvement of NF-κB pathway. *Eur J Pharmacol* 2008; **584**(1): 159-165.

[29]Zhong WT, Wu YC, Xie XX, Zhou X, Wei MM, Lanan Wassy S, et al. Phillyrin attenuates LPS-induced pulmonary inflammation *via* suppression of MAPK and NF-κB activation in acute lung injury mice. *Fitoterapia Milano* 2013; **90**(90): 132-139.

[30]Wang NP, Geng CP, Sun HY, Wang X, Li FM, Liu XC. Hesperetin ameliorates lipopolysaccharide-induced acute lung injury in mice through regulating the TLR4-MyD88-NF-kappaB signaling pathway. *Arch Pharm Res* 2019; **42**(12): 1063-1070.

[31]Ding YH, Miao RX, Zhang Q. Hypaphorine exerts anti-inflammatory effects in sepsis induced acute lung injury *via* modulating DUSP1/p38/JNK pathway. *Kaohsiung J Med Sci* 2021; **37**(10): 883-893.